PHYSICAL REVIEW B

SOLID STATE

THIRD SERIES, VOL. 2, NO. 3 1 AUGUST 1970

Rotary Saturation of the Nuclear Magnetic Resonance of ^{57}Fe in Pure Fe Metal

E. F. Mendis* and L. W. Anderson

Department of Physics, University of Wisconsin, Madison, Wisconsin 53706

(Received 19 September 1969)

Rotary saturation of the nuclear magnetic resonance of ^{57}Fe in pure Fe metal has been studied at room temperature and at 77 °K. The relative decrease of the amplitude of the nuclear-magnetic-resonance signal is plotted as a function of the frequency of the audio-frequency field producing the rotary saturation. A qualitative analysis of the rotary saturation data, obtained at different values of the applied rf field, provides the following information: There is a distribution of enhancement factors in the Fe sample. The distribution of enhancement factors is independent of temperature. The maximum enhancement factor in the sample studied is ~ 9000. These results are discussed with reference to other published research on the enhancement factors in Fe metal.

I. INTRODUCTION

In the past decade, Redfield reported a novel effect, which he called rotary saturation.[1] This effect may be described in the following way: When a spin system is subjected to an intense rf magnetic field, the steady-state nuclear magnetization will be parallel to H_e, the effective field in the rotating frame. If an oscillatory field (having a component perpendicular to H_e) is applied at the frequency $\omega_a = \gamma H_e$, then transitions will be induced and the magnetization parallel to H_e will be decreased. This nuclear resonance in the rotating frame is called rotary saturation. If the experimental conditions are such that the resonance condition is satisfied in the static frame, then the rotary saturation occurs when $\omega_a = \gamma H_1$, where H_1 is the magnitude of the rotating component of the rf field at the nucleus. Therefore, rotary saturation provides a convenient method of measuring H_1.

Portis and Gossard[2,3] observed nuclear magnetic resonance (NMR) in a ferromagnetic sample Co. They found that the power absorbed by the ferromagnetic sample was very large and included a term proportional to the dispersion part of the nuclear susceptibility. The large absorption of power was shown to occur because the rf magnetic field at the nucleus was a factor of 10^3–10^4 greater than the applied rf field.[3] This large enhancement was found to result from the motion of the domain walls. As the rf field drives a domain wall, the electronic spin of an atom located in the wall is rocked back and forth providing a large rf field which is perpendicular to the static hyperfine field.[3]

Gossard, Portis, Rubinstein, and Lindquist[4] have derived a theoretical expression showing that the contribution of the nuclear dispersion to the power absorbed by the ferromagnetic sample results from a modulation of the domain wall losses by the nuclear susceptibility driven by the enhanced rf field.

Other work has shown that similar results are obtained with Fe [5-8] and Ni [9-11] samples.

Rotary saturation has been applied to the NMR of nuclei in ferromagnetic materials in order to measure the enhancement of the rf field.[11,12] This paper reports a study of the rotary saturation of the NMR of ^{57}Fe in very pure Fe metal. The results of this study indicate that there is a distribution of enhancement factors present in an Fe sample. The distribution of enhancement factors is independent of temperature. The results of this study will be discussed in relation to the results of other workers.

II. APPARATUS

The sample used for this experiment was a powder prepared from zone-refined Fe. The sample was provided for us by the University of Wisconsin,

Department of Minerals and Metals Engineering. The sample had a purity of about 99.995%. The principal impurities in parts per million (by weight) were Co – 10 ppm, Cr – 10 ppm, Ge – 1 ppm, Mg – 1 ppm, Cu – 2 ppm, Mn – 1 ppm, C – 1 ppm, Ta – ≤3 ppm, Mo – 4 ppm, S – ≤3 ppm, O – 1 ppm, Si – ≤1 ppm, K – 3 ppm, and Ni – ≤4 ppm. All other impurities were well below 1 ppm. The analysis was carried out with a mass spectrometer after the sample was prepared. The bulk sample after zone refining had a maximum resistivity ratio with a magnetic field of $\rho\,(297 \pm 1.5)\,^{\circ}\mathrm{K}/\rho\,4.2\,^{\circ}\mathrm{K} = 630$. The powder sample was annealed so as to eliminate cold work. The individual Fe particles of our sample had a wide range of sizes and shapes, the largest size being about 40 μ.

The NMR of ^{57}Fe metal utilizes the internal hyperfine field at the ^{57}Fe nucleus. The NMR frequency of ^{57}Fe in pure Fe occurs at about 45 MHz. This frequency is too high for some oscillator circuits. Because the NMR utilizes the internal hyperfine field the oscillator frequency must be swept in order to traverse the resonance, and the oscillator must be frequency modulated so that phase-sensitive detection can be used.

The oscillator used in these experiments was a modified version of one designed by Knight.[13] Although Knight's original circuit was designed to operate at 2–10 MHz the rf amplification and feedback circuits are easily modified so that the circuit will operate at 45 MHz. The oscillator is a limiting type of oscillator; it operates at high rf levels and is sensitive only to power absorbed. The tank circuit of the oscillator consists of a variable air capacitor, an inductor within which the sample is placed, and a device for frequency modulation. When the oscillator is modulated at only one frequency ω_m, for example, in plotting the hyperfine field spectra of Fig. 1, the modulation

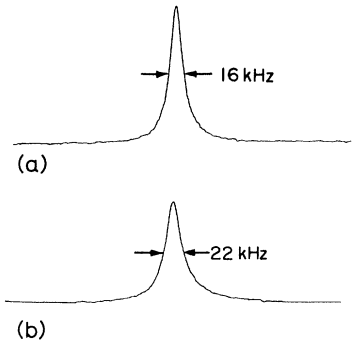

FIG. 1. Distribution of hyperfine fields in pure Fe metal (a) $T = 295\,^{\circ}\mathrm{K}$, (b) $T = 77\,^{\circ}\mathrm{K}$. In both traces $\omega_m/2\pi = 350$ Hz, $\gamma H_m/2\pi = 10^3$ Hz, and $H_x/2$ is less than 10^{-3} G. Horizontal scales in the two traces are not the same.

was obtained by coupling in parallel with the tank capacitor a small capacitor consisting of one fixed plate and one plate driven by a small audio speaker. When an audio-frequency signal is applied to the speaker the plate separation varies with the audio signal, thus providing a frequency-dependent capacity in the tank circuit. This device is not satisfactory for the relatively high-frequency modulation required for rotary saturation ($\omega_a \sim 10^5\ \mathrm{sec}^{-1}$). For this purpose a dc back-biased diode (a varicap) was coupled into the tank circuit and both the modulation signals ω_m and ω_a were applied simultaneously as ac on top of the dc bias voltage.

The frequency of the oscillator is swept by driving the air capacitor in the tank with a synchronomator. In order to obtain a plot of the hyperfine fields the oscillator frequency is slowly tuned through the ^{57}Fe NMR. As the oscillator is tuned the audio output signal is amplified and recorded using phase-sensitive detection locked to the fundamental modulation frequency. The output time constant of the detector was 1 sec. Direct comparison of the phase between the audio signal and the signal used for phase-sensitive detection was made using a dual beam oscilloscope. The phase-sensitive detection was set to be in quadrature with ω_m.

In order to obtain the rotary saturation data, exactly the same detection procedure was used. The resonance line was first plotted with zero amplitude of the modulation at the frequency ω_a, then plotted again with the second modulation applied, and then once more without any modulation. This procedure ensured that small changes in the signal intensity due to rotary saturation would be detected, and eliminated intensity changes due to spurious experimental effects. The smallest changes in signal intensity that can be detected depend upon the stability of the whole spectrometer. In these experiments, a precision of at least 10% could be maintained long enough to obtain all the data points such as those in Fig. 2. The low-temperature data were obtained in the same manner, with the inductor containing the sample immersed in a bath of liquid nitrogen.

The applied rf field produced by the inductor in the oscillator tank circuit was plotted out using an inductively coupled probe (care was used to assure that the capacitative coupling of the probe was very small). The probe consisted of several turns of wire on a hollow cylindrical form. The emf induced in the probe by the alternating rf magnetic field of the oscillator tank circuit was measured. The magnetic field was then calculated from this emf and the known geometry. The measurements were made with the sample in the coil (and inside the hollow probe form). The rf field was very

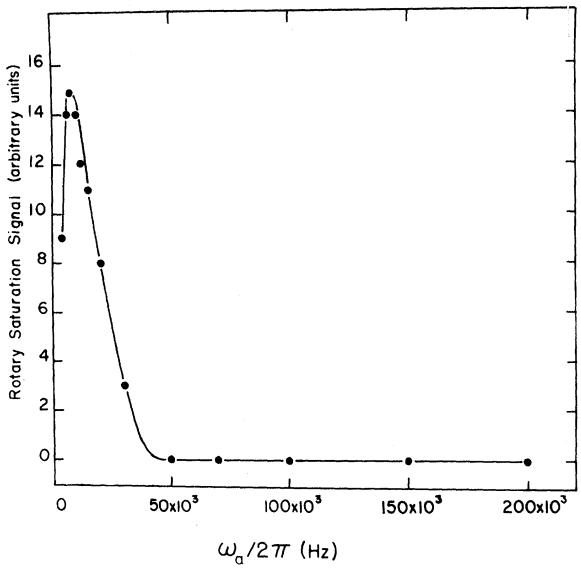

FIG. 2. Rotary saturation signal (RSS) as a function of $\omega_a/2\pi$. For this plot $H_x/2 = 30\times10^{-3}$ G, $T = 295\,^{\circ}$K, $\gamma H_a/2\pi \approx 4.5\times10^3$ Hz, and $\gamma H_m/2\pi \approx 2\times10^3$ Hz. Black points are experimental data and solid line is merely a smooth curve through the data points. Note that RSS $= 0$ for $\omega_a/2\pi > 50\times10^3$ Hz. Precision of each datum point is estimated to be about 15% of maximum value of rotary saturation signal.

homogeneous across a diameter of the coil ($\leq 10\%$ variation). Along the axis of the coil, the field was a maximum at the center of the coil and fell slowly to a value at the end of the coil of about 0.7 times the value at the center of the coil. The value of the rf field over the sample varied by no more than about 15%. The field at the center of the coil as measured using the probe agreed with the value computed from the measured voltage across the coil of the tank circuit to within 10%. (Note both the voltage across the oscillator tank coil and emf induced in the probe can be used to calculate an average oscillating magnetic field B in the tank coil without knowing the susceptibility μ of the sample. This field B is assumed to drive the domain walls. Later in this paper we shall use a microscopic picture and shall not distinguish between B and H.)

III. EXPERIMENTAL OBSERVATIONS

Figure 1 shows the distribution of hyperfine fields in our particles at room temperature 295 °K, and at 77 °K. These distributions of hyperfine fields were taken with the phase-sensitive detection in quadrature with the modulation and utilizing the fast passage effects which occur in the NMR of ^{57}Fe in pure Fe metal as discussed by Cowan and Anderson.[8,14,15] The distribution of hyperfine fields observed is almost symmetric at both 295 and 77 °K, and the line shape is nearly Lorentzian except that the wings are not as intense as the wings of a Lorentzian curve. The half-width at half-maximum of the line is $\Delta\omega/2\pi = 8\times10^3$ Hz at 295 °K and is $\Delta\omega/2 = 11\times10^3$ Hz at 77 °K. These results, obtained using extremely pure Fe, are the same as have been previously observed for an Fe sample prepared from carbonyl Fe by a process that removes the C and O impurities from the carbonyl Fe.[8] This indicates that the linewidth is probably not a strongly structure-sensitive quantity.

The rotary saturation experiments may be described as follows.[1,16] A linearly polarized rf magnetic field $2H_1\cos\omega t$ is applied to a nucleus at right angles to the static hyperfine field H_n. The linearly polarized field is composed of two oppositely rotating components. Only one of the two rotating components is effective in inducing transitions between the Zeeman levels of a nuclear spin. The other component can be neglected unless H_1 is comparable to H_n. In a coordinate system rotating with an angular velocity which is equal to the instantaneous frequency ω and rotating in the sense of the circularly polarized component which can induce transitions, the nuclear spin experiences a time-independent effective field, $\vec{H}_e = (H_n - \omega/\gamma)\vec{k} + H_1\vec{i}$. When H_1 is sufficiently large, the nuclear magnetization orients itself along H_e, precessing about H_e with frequency $\omega_a = \gamma H_e$.[1,15,16] If ω is near γH_n, then $\vec{H}_e \approx H_1\vec{i}$ and the nuclear magnetization is approximately at right angles to the static field H_n.

If another alternating field $H_a\cos\omega_a t\vec{k}$ is applied to the system, the magnetization, which is now parallel to H_e, is altered. This effect can be most easily understood by transforming to a second rotating frame, while considering H_e as the static field. When $\omega_a = \gamma H_e$, transitions are induced by the second oscillating field (which has a component perpendicular to H_e) and the magnetization along H_e is reduced. This, of course, will alter χ' and the signal observed in the static frame will be altered. This effect is rotary saturation. The value of H_a was usually set so that $\gamma H_a/2\pi \approx 5\times10^3$ Hz and was maintained at the same level as ω_a was varied. The relaxation time for ^{57}Fe in pure Fe metal at $T = 295\,^{\circ}$K is approximately $T_1 = 0.25\times10^{-3}$ sec.[7] Consequently, $\gamma H_a T_1 \approx 2\pi\times5\times10^3\times0.25\times10^{-3} = 7$. For a typical value $\gamma H_1/2\pi \approx 20\times10^3$ Hz one can be off resonance by approximately 140×10^3 Hz and still satisfy the condition that $\gamma H_{a\perp} T_1 > 1$, where $H_{a\perp}$ is the component of H_a perpendicular to H_e. Since the inhomogeneous linewidth is $\Delta\omega/2\pi = 8\times10^3$ Hz at room temperature all the spin packets in the entire inhomogeneous line satisfying the condition $\omega_a = \gamma H_e$ are saturated.

In a material like Fe, the time-dependent field

acting on a nuclear spin depends on the domain wall enhancement. Thus if the field produced by the oscillator $H_x \cos\omega t$ is determined and the time-dependent field at the nucleus $2H_1 \cos\omega t$ is measured by rotary saturation one can ascertain the domain wall enhancement factor.

In our ferromagnetic sample, it is impossible to apply an alternating field parallel to H_n. However, the Z component of the field in the rotating coordinate system is $(H_n - \omega/\gamma)$, and so a modulation of ω is entirely equivalent to a modulation of the magnetic field along the Z axis.[1,15-17] In this experiment we sweep across the nuclear resonance line while weakly modulating the oscillator frequency ω to provide a signal for the lock-in detector. We detect the signal in quadrature with this modulation. In addition, ω is modulated with a second frequency ω_a to provide the alternating magnetic field for the rotary saturation. We then measure the decrease in amplitude of the NMR signal at the center of the resonance line and divide this by the amplitude of the NMR signal when the second alternating field is not applied. This quantity we call the rotary saturation signal.

Figures 2 and 3 show plots of the rotary saturation signal at room temperature as a function of $\omega_a/2\pi$ at two different applied rf levels, $H_x/2 = 30\times10^{-3}$ G and $H_x/2 = 77\times10^{-3}$ G, respectively. In both these traces the slow modulation, used to provide a signal for the lock-in detection, was applied at $\omega_m = 325$ Hz.

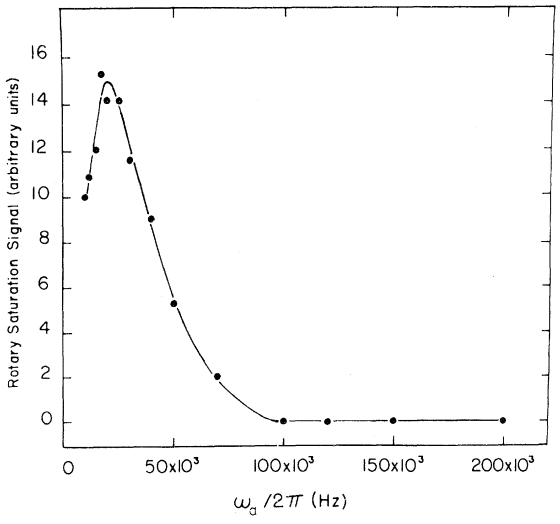

FIG. 3. Rotary saturation signal (RSS) as a function of $\omega_a/2\pi$. For this plot $H_x/2 = 77\times10^{-3}$ G, $T = 295$ °K, $\gamma H_a/2\pi \approx 4.5\times10^3$ Hz, and $\gamma H_m/2\pi = 2\times10^3$ Hz. Black points are experimental data and solid line is merely a smooth curve through data points. Note that RSS $= 0$ for $\omega_a/2\pi \geq 100\times10^3$ Hz.

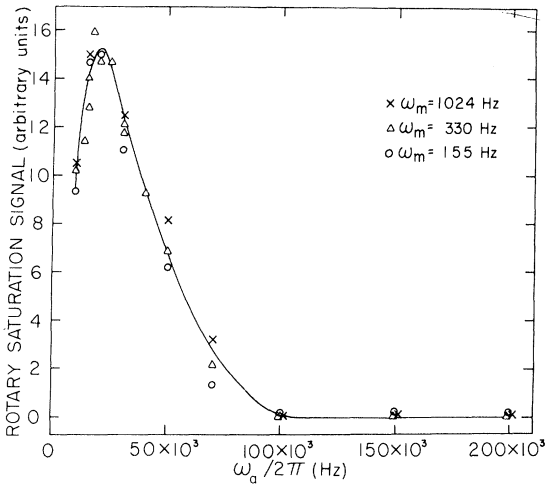

FIG. 4. Rotary saturation signal as a function of ω_m. For these data, ω_m has the values 155 Hz (○), 330 Hz (Δ), and 1024 Hz (X). Data were taken with $H_x/2 = 77\times10^{-3}$ G and $T = 295$ °K. Solid line is merely a smooth curve through the data. Note that rotary saturation signal has no obvious dependence on ω_m within our accuracy which was about ±15% of maximum value of rotary saturation signal.

In Fig. 4 the effect of varying the slow modulation frequency ω_m on the rotary saturation signal is shown. It is seen that the rotary saturation signal depends only weakly on the modulation frequency over the range of ω_m from 155 to 1024 Hz. These data were all taken at room temperature.

Data similar to these were obtained at several rf levels. Figure 5 shows a plot of the value of

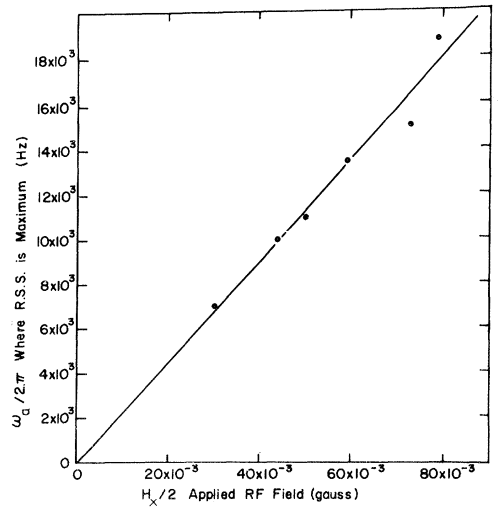

FIG. 5. Frequency $\omega_a/2\pi$ when rotary saturation signal (RSS) is a maximum versus applied rf field $H_x/2$. For this plot $T = 295$ °K. Slope of solid line implies $\eta_{av} = 1700$ as discussed in text.

$\omega_a/2\pi$ at which the rotary saturation signal reaches a maximum versus $H_x/2$, the rotating component of the applied rf field. It is observed that this plot can be fitted by a straight line through the origin. The half-width of the plot of the rotary saturation data versus $\omega_a/2\pi$ was also approximately proportional to $H_x/2$. The half-width from the maximum to half-height on the high-frequency side of the plot at $H_x/2 = 30\times10^{-3}$ G was $\Delta\omega_a/2 \approx 13\times10^3$ Hz, and the width at $H_x/2 = 77\times10^{-3}$ G was $\Delta\omega_a/2 \approx 30\times10^3$ Hz. These two observations are consistent with rotary saturation occurring when $\omega_a = \gamma H_1$ and with a distribution of enhancement factors relating H_1 and H_x (as discussed in Sec. IV of this paper).

Figure 6 shows a plot of the rotary saturation signal at 77 °K versus $\omega_a/2\pi$ for an applied rf field of $H_x/2 = 77\times10^{-3}$ G and at $\omega_m = 325$ Hz. Comparison of Figs. 3 and 6 shows that the two plots, at 77 °K and at room temperature, with $H_x/2 = 77\times10^{-3}$ G are very similar. It was found that the results at 77 °K were all very similar to those at room temperature. We conclude that the value of the enhancement factors and the distribution of enhancement factors are nearly independent of temperature for our sample.

The signal observed as we swept across the resonance line was symmetric about $\omega = \omega_0$ for all values of ω_a and H_a. The line shape observed did, of course, depend on both H_a and ω_a. As H_a increased the observed static frame NMR signal at ω_0 decreased. As ω_a was varied with H_a set at a relatively low value, the observed NMR signal was affected most strongly near $\omega = \omega_0$ at low values of ω_a, and then the line shape was altered symmetrically on both sides of ω_0 as ω_a was increased. These effects can be understood by considering the nuclear resonance in the rotating frame. The effect of the second modulating frequency is to decrease or eliminate the contribution to the signal of those nuclear moments near $(\omega - \omega_0) = \pm[\omega_a^2 - (\gamma H_1)^2]^{1/2}$. Thus when $\omega_a = \gamma H_1$ the amplitude of the resonance line is reduced most at $\omega = \omega_0$. However, as ω_a increases the maximum decrease in the signal occurs at two frequencies, one on either side of ω_0. The observed symmetry in the signal indicates that any frequency dependence in η, the enhancement factor relating H_1 and the applied field H_x, must also be symmetric about ω_0. It seems logical to make the simplest assumption, which is that η is independent of ω at least over the frequency range immediately surrounding $\omega = \omega_0$. With a distribution of enhancement factors, the observed symmetry of the signal for all ω_a and H_a indicates that the frequency dependence of the distribution of enhancement factors must be symmetric about ω_0.

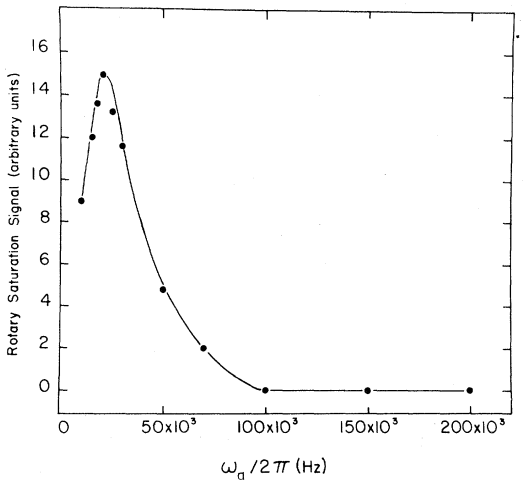

FIG. 6. Rotary saturation signal (RSS) as a function of $\omega_a/2$. For this plot $H_x/2 = 77\times10^{-3}$ G, $T = 77$ °K, $\gamma H_a/2 \approx 4.5\times10^3$ Hz, and $\gamma H_m/2 \approx 2\times10^3$ Hz. Black points are experimental data and solid line is merely a smooth curve through data points. Note that RSS $= 0$ for $\omega_a/2\pi \geq 100\times10^3$ Hz.

IV. DISCUSSION

We have attempted a detailed analysis of the rotary saturation data presented in the previous section. In principle this can be done in a straightforward manner. One calculates the static frame NMR signal that results from a signal spin. One must then average this signal over the random orientation of the applied rf field with respect to the domain walls, as discussed by Stearns.[18] After this, one must average over the distribution of resonant frequencies for the individual spins.[15] Next, one must average over a distribution of enhancement factors η and over the distribution of relaxation times.[18,19] The distribution of relaxation times may be correlated with the distribution of enhancement factors,[19] i.e., the spins in a particular domain wall that have the largest enhancement factor also will probably have the shortest relaxation time. If the correlation of the enhancement factors and relaxation times are treated correctly then one will have an expression for the NMR signal observed. One now must calculate how this signal will change when one applies the rotary saturation field.[1,16] This calculated rotary saturation signal and the experimental rotary saturation data can in principle be utilized to yield the distribution of enhancement factors and the correlation between η and T_1 in our sample.

We have made calculations of the type described. However, these calculations can not be used to extract a unique expression for the distribution of enhancement factors without an order-of-magni-

tude increase in the precision of the experimental data. Since our errors are less than ± 10% of the maximum value of the rotary saturation signal, a large increase in the precision is beyond our capabilities at the present time. Nevertheless, the experimental data do provide significant information. We shall discuss those aspects of the data that can be obtained from a qualitative analysis.

The first observation on the rotary saturation data is that it does imply a distribution of enhancement factors. In order to see this let us first try to explain the slow fall from the maximum rotary saturation signal as ω_a increases. Since the NMR signal of ^{57}Fe in pure Fe metal is inhomogeneously broadened, the inhomogeneous broadening will contribute to the width of the rotary saturation data. By considering the resonating nuclei in the rotating frame it is easily seen that the contribution $\delta\omega$ to the width of the rotary saturation signal from the inhomogeneous linewidth is much too small to explain the entire width of the rotary saturation signal. If γH_1 is large compared to the inhomogeneous linewidth $\Delta\omega$, then the rotary saturation without a distribution of enhancement factors can extend only from $\omega_a = \gamma H_1$ to $\omega_a \approx \gamma H_1 + (\Delta\omega)^2/2\gamma H_1$ so that $\delta\omega = (\Delta\omega)^2/2\gamma H_1$. Since $\Delta\omega = 8$ kHz at $T = 300\,^\circ$K this implies that $\delta\omega \leq 2$ kHz for the high rf-level data where $\gamma H_1 > 20$ kHz. The rotary saturation data of Figs. 3, 4, and 6 are obviously much broader than this. Also, as was previously pointed out, the width of the rotary saturation data is proportional to the applied field H_x. These considerations lead one to the conclusion that for $\omega_a \geq 20$ kHz the width of the rotary saturation data must be due almost entirely to a distribution of enhancement factors.

The maximum value of the enhancement factor η_{max} observed in our sample can be calculated from Fig. 3, Fig. 4, or Fig. 6. It is $\eta_{max} = (\omega_a)_{max}/\frac{1}{2}\gamma H_x \approx 9000$, where we have used 9.5×10^4 as the highest frequency for which we observe a nonzero rotary saturation signal. The value of η_{max} is independent of the temperature.

From the slope of the line in Fig. 5 one can obtain an estimate of an average enhancement factor for the nuclear spins producing the NMR signal of ^{57}Fe in pure Fe metal. This is obtained by writing $\omega_a = \gamma H_1 = \gamma \eta_{av} H_x/2$. The average enhancement factor, obtained using this equation as the definition of η_{av} is $\eta_{av} \approx 1700$. (Note: This definition of η_{av} already includes an average over the random direction of H_x relative to the domain magnetization. The average enhancement factor would be about $\eta_{av} \approx 3400$ if H_x were applied only along the direction of the domain magnetization.)

The average enhancement factor $\eta_{av} = 1700$ as measured from the maximum of the rotary saturation signal is consistent with the measurements of Robert and Winter[6] and Cowan and Anderson.[8] Obviously the static NMR signal is strongly influenced by enhancement factors of this magnitude.

The fact that the shape of rotary saturation signal is nearly independent of the modulation frequency ω_m is significant. It can be shown that both the NMR signal and the rotary saturation signal as detected in fast passage and detected 90° out of phase with the modulation vary as $\omega_m T_1/[1+(\omega_m T_1)^2]$. If T_1 is strongly dependent on η then the shape of the rotary saturation signal will depend on ω_m. Therefore, this experiment indicates that T_1 and η are *not* strongly correlated. A theory such as that of Winter[20] would have indicated that $T_1 \propto \eta^{-2}$. We have very carefully inspected our data using the range of values of T_1, given by Stearns[19] and conclude that our data plainly rule out the possibility that $T_1 \propto \eta^{-2}$. Whatever causes the distribution of enhancement factors does not cause the corresponding distribution of relaxation times. This is consistent with the results of Stearns[18,19] who concluded that T_1 was equal to $k(d\theta/dz)^2$ where k is a constant, but that $(d\theta/dz)^{-1}$ was only one of the causes of the distribution of enhancement factors in her sample (θ is the angle of an electronic spin at position z in the wall relative to the direction of the domain magnetization).

In an interesting recent experiment Stearns[18] has studied the enhancement factors in pure Fe metal. She concluded that there was a distribution of enhancement factors, and that this distribution of enhancement factors resulted from the distribution of angles between H_x and the domain magnetization, the variation of $d\theta/dz$ through the domain wall, the assumption that the domains are in the shape of a drumhead being bound around the perimeter, and the assumption that the areas of the drumheads varied from one wall to the next. She further found that the distribution of enhancement factors was strongly temperature dependent. In addition, she observed unexplained asymmetries in her spin echo NMR experiments on Fe.

In our experiments we find that our value of $\eta_{max} \sim 9000$ is in good agreement with Stearns's value of $\eta_{max} \sim 8500$ at $T = 78\,^\circ$K.[18] However, we obtain $\eta_{max} \sim 9000$ at 300 °K, whereas Stearns obtains 19 000. Thus we do not detect the temperature dependence of η_{max} found by Stearns. Although as previously pointed out we have not been able to invert our data to yield the distribution of enhancement factors, we have been able to utilize the particular distributions of enhancement factors[18] and variation of T_1 [19] through the domain walls given by Stearns and calculate the shape of the rotary saturation data. To within the precision of our data, the drumhead model of Stearns can be used to fit our observations. Stearns's model, of

course, fits only the shape of the rotary saturation data as a function of η/η_{max} and does not explain why η_{max} is different in this experiment from that in her experiment. (Stearns[18] did not invert her data in order to obtain the distribution of enhancement factors either, but instead merely showed that her drumhead model fit the experimental data.) The fact that our data can be fitted by Stearns's model lends support to Stearns's hypothesis that the distribution of enhancement factors arises not only from the averaging over the random angle between H_x and the domain magnetization and the variation of $d\theta/dz$ through the domain wall but also may include a contribution that would arise were the domain walls bound around the perimeter like a drumhead. However, we do not believe that one can conclude that this is the only possible mechanism for producing the distribution of enhancement factors, i.e, there is no evidence that Stearns's drumhead model is the only model that will fit our data. Portis *et al.*[3,4] have calculated the enhancement factor for a spherical particle divided by a single 180° domain wall. The enhancement factor was found to be about $\eta = 1200-1800$ and the enhancement factor was found to vary inversely with the demagnetizing factor ($4\pi/3$ for the spherical particle). Since our particles have a variety of shapes, one might expect that the demagnetizing factors would vary from 4π down to nearly zero. This would lead to a distribution of enhancement factors. Although the drumhead model explains adequately the distribution of enhancement factors it does not indicate why η_{max} should be so much larger than the value calculated by Portis *et al.* The possibility that the distribution of enhancement factors is due to the variation of demagnetizing fields does explain this. It would be interesting to see what results would be obtained if one could measure the distribution of enhancement factors in small spherical particles containing only one domain wall.

In addition, there are two types of domain walls[21] in Fe; 90° walls and 180° walls, made up of two 90° walls back-to-back. Stearns concluded that her sample contained only 180° walls; however, the relative ratio of the two types of walls in a sample may depend on the details of closure and hence on the size and shape of the particles. A magnetic field H_x will produce a different response when acting on a 90° wall than on a 180° wall and, hence, this may also contribute to the distribution of enhancement factors.

We do *not* see any asymmetries in either the static frame NMR or in the effect of rotary saturation on the NMR line shape. We conclude that the mysterious asymmetries observed by Stearns[18] were probably due to instrumental effects and we see no reason to believe that NMR is not a satisfactory method for studying the hyperfine fields in alloys. In this we are in agreement with Rubinstein[22] and Murphy *et al.*[23] and in disagreement with Stearns.[18]

The results of this experiment are summarized and compared with the results of Stearns[18] in Table I.

Finally, we should like to comment that the use of the fast passage effects (as reported by Cowan and Anderson[8,11] and as used by Rubinstein *et al.*[22,24] and Mendis and Anderson[25]) to plot out directly the distribution of hyperfine fields in ferromagnetic materials is not affected by the distribution of enhancement factors provided the conditions are chosen satisfactorily. This result is obvious if one realizes that for a fixed η the NMR signal is just the distribution of hyperfine fields. Consequently, after averaging over η, the observed NMR signal is still simply the distribution of hyperfine fields.

TABLE I. Comparison of major results of this experiment with experiment of Stearns.

	Stearns (Ref. 18)	This experiment
η_{max} (77 °K)	8 500	9000
η_{max} (room temp.)	19 000	9000
η_{av}	...	1700
Do data imply a distribution of η's[a]	Yes	Yes
Do asymmetries of unknown origin occur in NMR line shapes for ^{57}Fe in Fe metal	Yes	No
Can NMR be used to study detailed line shapes in Fe alloys	No	Yes

[a]Stearns has interpreted the distribution of enhancement factors as resulting from a distribution of angles between H_x and the domain magnetization, a variation of $d\theta/dz$ through the domain wall (where θ is the angle between the electronic spin direction and the domain magnetization at the position z in the domain wall), and from the assumption that the domain walls are bound around the perimeter like a drumhead. Stearns has concluded that the drumhead model for the domain wall will lead to a strong temperature dependence of the maximum value of the enhancement factor, and that the drumhead model may explain the mysterious asymmetries observed in the NMR line shapes in ferromagnetic materials. In the present experiment we do not observe the temperature dependence of the maximum value of the enhancement factor or the mysterious asymmetries in the line shapes. The data on the relative distribution of enhancement factors in our experiment can be explained by Stearns's drumhead model. However, we believe that these data can also be explained by a distribution of demagnetizing factors in our particles. A distribution of demagnetizing factors may also explain why the maximum value of the enhancement factor is as large as 9500 since small demagnetizing factors will produce large enhancements when coupled with Portis's theory of enhancement factors.

ACKNOWLEDGMENTS

The authors would like to thank Professor R. A. Dodd of the University of Wisconsin, Department of Minerals and Metals Engineering for providing the zone-refined Fe sample and its analysis. The authors would also like to acknowledge many helpful discussions with Professor P. R. Moran, Professor D. L. Huber, and Professor M. E. Ebel.

---

*Present address: Department of Physics, University of New Brunswick, Fredricton, New Brunswick, Canada.

[1]A. G. Redfield, Phys. Rev. 98, 1787 (1955).

[2]A. C. Gossard and A. M. Portis, Phys. Rev. Letters 3, 164 (1959).

[3]A. M. Portis and A. C. Gossard, J. Appl. Phys. 31, 205S (1960).

[4]A. C. Gossard, A. M. Portis, M. Rubinstein, and R. H. Lindquist, Phys. Rev. 138, A1415 (1965).

[5]A. C. Gossard, A. M. Portis, and W. J. Sandle, Phys. Chem. Solids 17, 341 (1961).

[6]C. Robert and J. M. Winter, Compt. Rend. 250, 3831 (1960).

[7]J. I. Budnik, L. J. Bruner, R. J. Blume, and E. L. Boyd, J. Appl. Phys. 32, 120S (1961).

[8]D. L. Cowan and L. W. Anderson, Phys. Rev. 135, A1046 (1964).

[9]L. H. Bruner, J. I. Budnik, and R. J. Blume, Phys. Rev. 121, 83 (1961).

[10]R. L. Streever and L. H. Bennett, Phys. Rev. 131, 2000 (1963).

[11]D. L. Cowan and L. W. Anderson, Phys. Rev. 139, A424 (1965).

[12]D. L. Cowan, Ph.D. thesis, University of Wisconsin at Madison, 1964 (unpublished).

[13]W. D. Knight, Rev. Sci. Instr. 32, 95 (1961).

[14]A. M. Portis, Phys. Rev. 100, 1219 (1955).

[15]A. M. Portis, Sarah Mellon Scaife Radiation Laboratory, University of Pittsburgh, Technical Note No. 1, 1955 (unpublished); also M. Weger, Bell System Tech. J. 39, 1013 (1960); G. Feher, Phys. Rev. 114, 1219 (1959).

[16]A. Abragam, *Principles of Nuclear Magnetism* (Oxford U. P., London, England, (1961).

[17]P. R. Moran, J. Phys. Chem. Solids, 30, 297 (1969).

[18]M. B. Stearns, Phys. Rev. 162, 496 (1967); see also M. B. Stearns and A. W. Overhauser, J. Appl. Phys. 39, 4355 (1968).

[19]M. B. Stearns, Phys. Letters 27A, 706 (1968).

[20]J. M. Winter, Phys. Rev. 124, 452 (1961).

[21]C. Kittel and J. K. Galt, *Solid State Physics* (Academic, New York, 1956), Vol. 3, p. 437.

[22]M. Rubinstein, Phys. Rev. 172, 277 (1968).

[23]J. J. Murphy, J. I. Budnik, and S. Skalski, J. Appl. Phys. 39, 1239S (1968).

[24]M. Rubinstein, G. H. Stauss, and J. Dweck, Phys. Rev. Letters 17, 1001 (1966).

[25]E. F. Mendis and L. W. Anderson, Phys. Rev. Letters 19, 1434 (1967).